Research Article
doi.org/10.1002/cplu.202100450
Chemistry Europe
European Chemical Societies Publishing

www.chempluschem.org

Peptide-Conjugated Silver Nanoparticles for the Colorimetric Detection of the Oncoprotein Mdm2 in Human Serum

Maurice Retout,[a] Bryan Gosselin,[a, b] Alice Mattiuzzi,[c] Indiana Ternad,[c] Ivan Jabin,*[b] and Gilles Bruylants*[a]

The development of efficient, reliable, and easy-to-use biosensors allowing early cancer diagnosis is of paramount importance for patients. Herein, we report a biosensor based on silver nanoparticles functionalized by peptide aptamers for the detection of a cancer biomarker, i.e. the Mdm2 protein. Silver nanoparticles (AgNPs) were produced and stabilized with a thin PEGylated-calix[4]arene layer that allows (i) the steric stabilization of the AgNPs and (ii) the covalent conjugation of the peptide aptamers via the formation of an amide bond. These peptide-conjugated AgNPs were then used to detect Mdm2 via a dual trapping strategy that was previously reported with gold nanoparticles (AuNPs). Our results showed that replacing AuNPs by AgNPs improves the detection limit by nearly one order of magnitude, down to 5 nM, while the high selectivity of the system and the stability of the particles provided by the calixarene coating allow the detection of Mdm2 in human serum.

Introduction

Cancer is a leading cause of death all around the world and development of new tools for its early diagnosis is crucial. Today, most of the cancer diagnosis are obtained via clinical imaging techniques that are not adapted to early diagnosis.[1–4] In this context, the use of biosensors to detect minute amount of cancer biomarkers in biological fluids appears as a promising strategy for the early diagnosis of cancer.[5]

The large majority of current medical diagnostic strategies target protein biomarkers[5–7] and are based on the enzyme-linked immunosorbent assay (ELISA).[8] However, despite its high sensitivity, this assay possesses significant drawbacks that limit its use in point-of-care settings, such as high production costs, complex procedures, and the need for trained operators.[9] The development of convenient, fast, cheap and sensitive methods allowing to detect small variations in protein levels in biological samples remains therefore of prime medical interest.

Due to their remarkable optical properties, systems based on plasmonic nanomaterials appear as a valuable alternative strategy for biomarker sensing. Plasmonic nanomaterials exhibit indeed a localized surface plasmon resonance (LSPR) band that, when falling in the visible region of the electromagnetic spectrum, can be exploited for colorimetric sensing.[10–12] Besides, their extinction coefficient is approximately three to four orders of magnitude higher than that of any organic molecule.[13,14] Gold nanoparticles (AuNPs) represent the vast majority[15] of the particles used in plasmonic nanomaterials-based biosensors because of their well-reported synthesis,[16] ease of surface functionalization[17–19] and good aqueous stability.[20] Those particles have been used for the sensing of a wide variety of analytes[21] ranging from small molecules[22,23] to proteins[24–27] and nucleic acids.[28,29] The most unambiguous detection signal is obtained from the aggregation or redispersion of the particles in presence of the analyte to detect. Aggregation of particles leads indeed to a coupling between their surface plasmons and a significant change in the extinction spectrum of the suspension.[30,31] This strategy however requires functionalizing the particles with ligands conferring them specificity for the selected analyte. Antibodies are the most frequent targeting ligands used with that objective.[32,33] However, the use of these biomolecules suffers from some severe drawbacks due to their large size that limits their number on a particle, reduces the LSPR band coupling by imposing a large distance between the metallic cores and renders their orientation at the particle surface difficult to control. These biomolecules furthermore present stability issues as well as large batch-to-batch variations.[34–36] To address these problems, synthetic affinity probes such as peptide aptamers have been considered in place of antibodies for the detection of biomolecules.[37,38] In comparison to antibodies, these are indeed far less expensive, easier to synthesize in a reproducible way as well as to manipulate and to conjugate onto surfaces with a controlled orientation. For this purpose, DNA and

[a] Dr. M. Retout, B. Gosselin, Prof. G. Bruylants
Engineering of Molecular NanoSystems
Ecole Polytechnique de Bruxelles
Université libre de Bruxelles
Avenue F. D. Roosevelt 50, CP165/64, 1050 Brussels (Belgium)
E-mail: Gilles.Bruylants@ulb.be
[b] B. Gosselin, Prof. I. Jabin
Laboratoire de Chimie Organique
Avenue F. D. Roosevelt 50, CP160/06, 1050 Brussels (Belgium)
E-mail: Ivan.Jabin@ulb.be
[c] Dr. A. Mattiuzzi, I. Ternad
X4C
Rue Auguste Piccard 48, 6041 Gosselies (Belgium)

Supporting information for this article is available on the WWW under https://doi.org/10.1002/cplu.202100450

peptide aptamers have been developed. If DNA aptamers are widely used thanks to the SELEX procedure that allows to identify DNA aptamers specific to almost any target molecule,[39] peptide aptamers show interesting properties, as the ability to use amino acids with much more functional groups than nucleic acids, their ease of synthesis and the possibility to identify their sequence from proteins able to form complexes with the target.

Mdm2 is a protein overexpressed in the early stages of the carcinogenesis. Thus, detection of abnormal concentrations of this oncoprotein would indicate the early formation of tumors that could be subsequently treated in time.[40] We recently developed a detection strategy of Mdm2 that involves a dual trapping mechanism: two sets of AuNPs bearing a different peptide aptamer are used to recognize Mdm2 in a ternary complex, whose formation induces the aggregation of the NPs.[41] High selectivity is ensured by the dual trapping mechanism, as a double recognition of the protein Mdm2 is required to trigger the aggregation. However, this system was based, as a vast majority of systems reported in the literature, on citrate capped AuNPs functionalized with peptide aptamers via a classical thiol chemistry and was thus lacking the necessary colloidal stability to work with biological samples.

From an optical sensing point-of-view, silver nanoparticles (AgNPs) appear to be better candidates than AuNPs as colorimetric reporters: for a given particle size, they exhibit an extinction coefficient which is approximately one order of magnitude higher than that of their Au counterpart.[42] Silver nanoparticles find many applications as Raman nanotags, in the biomedical field,[43,44] but also in food safety[45] and environmental monitoring.[46] In particular, picomolar determination of cytoplasmic and nuclear miRNAs in single living cells could be achieved using a plasmonic affinity sandwich assay[47] or the detection of cancer biomarkers achieved in spiked plasma samples using dual molecularly imprinted polymer-based plasmonic immune-sandwich assays.[48]

Our work focuses on the use of AgNPs in colorimetric aggregation-based assays, that presents the advantage of being detectable with the naked eye or with inexpensive equipment. The use of these assays with biological samples however represents a great challenge, as the colloids should remain stable in these complex environments in the absence of the target analyte. In this context, colorimetric aggregation-based biosensors (involving AgNPs) for the detection of a cancer biomarker in relevant working conditions are barely reported in the literature.[49] This absence of attention to AgNPs compared to AuNPs, despite better optical properties, is mainly due to their weak chemical stability and the difficulty to manipulate and conjugate them with biomolecules without leading to their degradation.[50-52] Indeed, if stable AgNPs have been obtained with thick organic coatings such as polymers[53,54] or plant extracts,[55,56] these AgNPs are however not suitable for colorimetric aggregation-based biosensors, as the interparticular distance in the aggregates remains large and hinders LSPR coupling. Therefore, AgNPs have mainly been reported for the simple detection of cationic species, as Cu^{2+},[57] Cr^{6+}[58] or Ca^{2+} (in the presence of cysteine),[59] or small molecular species[60]. In most cases however the receptor is immediately linked to the silver core by a thiol and the development of such sensors requires a case-by-case optimization of the silver nanoparticles functionalization conditions.

In this context, we recently developed ultra-stable and bioconjugable AgNPs coated with a thin layer of calixarenes[61,62] that represent a promising tool for the conception of biosensors.[63] These particles present excellent colloidal and chemical stabilities, as well as long-term shelf stability. In the continuity of our previous work on the colorimetric detection of the oncoprotein Mdm2,[41] we thus envisioned that these calixarene-coated AgNPs could advantageously replace the citrate-capped AuNPs that were used to develop this previously reporter system. This latter was based on the dual-trapping of the Mdm2 protein by two sets of AuNPs functionalized with peptides aptamers composed of the reported binding sequences of proteins p53[64] and p14[65] for the oncoprotein to which two cysteines were added at the N-term and C-term extremities respectively to ensure their attachment to the gold surface. This system proves to be selective for Mdm2 while ensuring a detection at a concentration as low as 30 nM but was not sufficiently stable to allow detection with biological samples.

Herein we report on the synthesis of ultra-stable silver nanoparticles stabilized with a thin PEGylated-calixarene layer (PEG-calix-AgNPs) and their covalent bioconjugation with peptide aptamers. These functionalized AgNPs were used for the detection of Mdm2 in human serum through a dual trapping strategy (Figure 1), paving the way for their use with real clinical samples.

Results and Discussion

Synthesis of the peptide-silver nanoparticles conjugates

PEGylated calixarene-coated silver nanoparticles with a narrow size distribution were synthesized by the reduction of silver

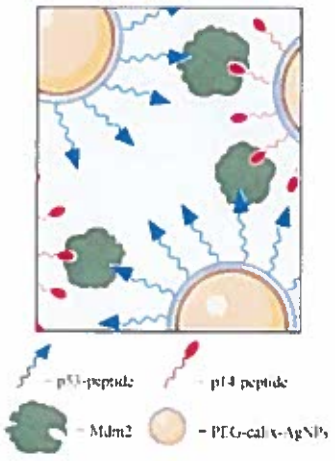

Figure 1. Illustration of the dual-trapping of Mdm2 by two sets of AgNPs coated by PEGylated calixarenes (PEG-calix-AgNPs), each conjugated to a peptide aptamer that recognizes a specific site of Mdm2.

nitrate in the presence of a PEGylated calixarene-tetradiazonium salt (PEG-calix-diazonium) via a recently reported procedure (Scheme 1) (see Experimental section for detailed procedure).[63] The calixarene used bears four PEG chains at the level of its small rim with one ended by a carboxyl group that allows the conjugation of peptides via the formation of an amide bond.[66] The PEG coating was selected to prevent the non-specific adsorption of endogenous proteins and, by stabilizing the particles sterically, minimize their sensitivity to ionic strength when used with biological samples.[67]

The colloidal and chemical stabilities of the resulting AgNPs were analyzed by absorption UV-Vis spectroscopy and compared to traditional AgNPs capped by citrate anions (citrate-AgNPs). It was observed that PEG-calix-AgNPs were stable in physiological conditions (pH 7, PBS 1x) and can be exposed to acidic conditions (pH 3) or potassium fluoride (150 mM) for several hours with only minor effects on colloidal stability and loss of AgNPs (Figure S1). In strong contrast, classical citrate-AgNPs can barely be centrifuged, not even once, and cannot endure acidic condition or even short exposure to potassium fluoride. These results confirm that the PEGylated calixarene layer, despite being thin, confers a high stability to the particles and allows to easily manipulate them (i.e. centrifugation or conjugation). This high stability allows them to be suspended in human serum for hours without showing signs of degradation or aggregation (Figure S2a). Furthermore, the PEG-calix-AgNPs do not express any variation of their LSPR band even 6 months after their synthesis (Figure S2b).

In a second step, the peptide aptamers were conjugated via the standard EDC/Sulfo-NHS procedure to the carboxyl groups protruding from the calixarene layer of the PEG-calix-AgNPs. Two distinct batches of peptide-conjugated AgNPs were produced, one with the p53 peptide aptamer (p53-PEG-calix-AgNPs) and another with the p14 peptide aptamer (p14-PEG-calix-AgNPs) (Scheme 1). After conjugation, the particles were cleaned with sodium dodecyl sulfate (SDS) to remove the physisorbed peptides. The minimal interaction sequences reported in the literature are colored in blue or red for p53[64] or p14,[65] respectively (Scheme 1). It is worth mentioning that the N-terminal extremity of the p14-peptide was acetylated in order to prevent its conjugation to the NP surface via this functional group as the interaction with Mdm2 is mainly due to the first 14 amino acids present at the N-terminal extremity of the peptide. Similarly, the side chain of the unique lysine residue of p53 was also protected.

p53-PEG-calix-AgNPs and p14-PEG-calix-AgNPs were characterized by UV-Vis and FTIR spectroscopies (Figure 2b–c). UV-Vis spectra of the peptide-conjugated AgNPs showed an intense LSPR band that was slightly broader than the LSPR band of PEG-calix-AgNPs. Mixing equimolar suspensions of the two batches gave rise to a stable suspension with a golden yellow color (Figure 2b, inset). It indicates that the two sets of particles do not interact with each other, despite bearing oppositely charged peptides. FTIR spectroscopy revealed the presence of amides I and II bands at 1650 and 1530 cm^{-1}, respectively, confirming the presence of the peptides on the particles. An intense band corresponding to the PEG chains (COC stretching at 1100 cm^{-1}) was also observed, indicating that the PEGylated calixarene layer was not removed during conjugation or during the subsequent cleaning steps (Figure 2c).

Mdm2 detection in buffer via the dual-trapping strategy

The detection of 30 nM of Mdm2 was first targeted as it was the detection limit for the previously reported AuNPs-based system.[41] The addition of 30 nM Mdm2 to an equimolar suspension of p53-PEG-calix-AgNPs and p14-PEG-calix-AgNPs in Tris.HCl buffer led to a rapid increase of the absorbance at 560 nm and to a decrease of the one at 490 nm, which is a clear signature of a DLCA type aggregation of the particles (Figure 3a).[68] After 30 minutes, barely no evolution of the LSPR band could be observed. The strong deformation of the LSPR band was associated to a clear change of color of the suspension from golden yellow to brown-orange, allowing naked eye detection (Figure 3a, inset).

Various control experiments were run to verify that the aggregation was indeed due to the selective double recognition of Mdm2 by the two types of peptide-conjugated AgNPs. The level of the aggregation was evaluated by measuring the ratios of the absorbances at 560 nm and 490 nm and by comparing it to the initial ratio of the p53-PEG-calix-AgNPs/p14-PEG-calix-AgNPs suspension ($\Delta = A_{560nm}/A_{490nm} - A^0_{560nm}/A^0_{490nm}$). No aggregation of the particles was observed when 30 nM of Mdm2 was added to either p53-PEG-calix-AgNPs, p14-PEG-calix-AgNPs or PEG-calix-AgNPs suspensions (Figure 3b).

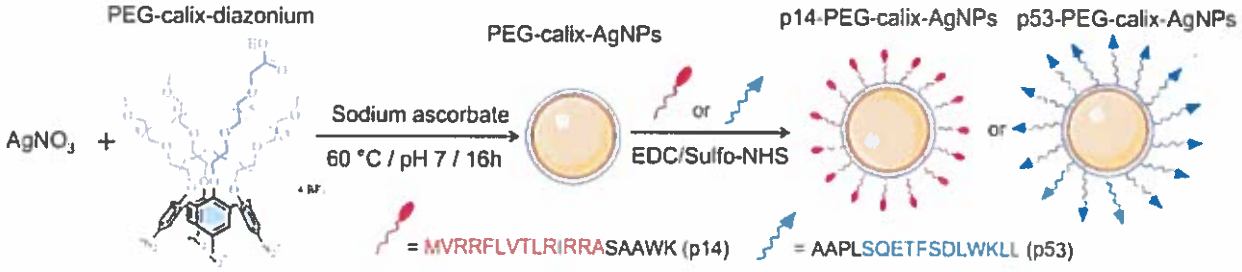

Scheme 1. Preparation of the peptide-AgNPs conjugates. Amino acids sequences of the p53-peptide and the p14-peptide necessary for the interaction with Mdm2 are labelled in blue or red respectively.

Research Article
doi.org/10.1002/cplu.202100450
Chemistry Europe
European Chemical Societies Publishing

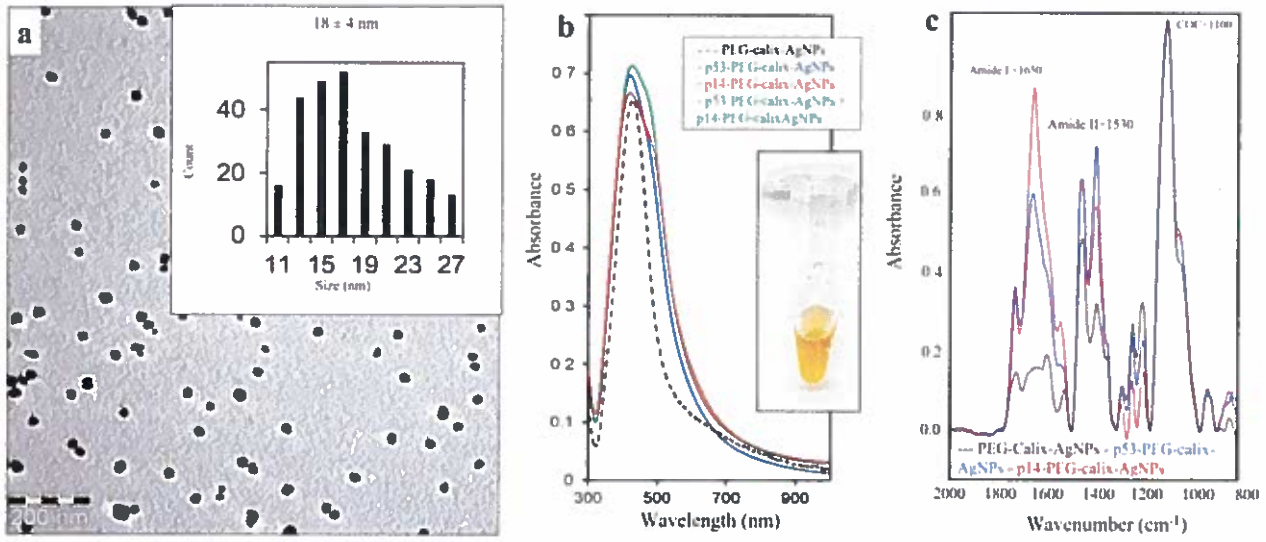

Figure 2. (a) TEM images of the PEG-calix-AgNPs. Inset shows the size distribution obtained by measuring the size of 300 AgNPs. (b) UV-Vis spectra of PEG-calix-AgNPs (black dashed line), p53-PEG-calix-AgNPs (blue plain line), p14-PEG-calix-AgNPs (red plain line) and equimolar mixture of p53- and p14-PEG-calix-AgNPs (green plain line) suspended in water. Inset shows a picture of equimolar mixture of p53- and p14-PEG-calix-AgNPs suspended in water (c) ATR-FTIR spectra of PEG-calix-AgNPs (black dashed line), p53-PEG-calix-AgNPs (blue plain line) and p14-PEG-calix-AgNPs (red plain line).

It clearly shows that (i) peptide conjugation and (ii) double recognition are mandatory to induce the aggregation. Besides, addition of Tris.HCl buffer as well as blood concentration of BSA (0.6 mM) did not induce any aggregation of the particles. The latter experiment confirms that the PEG layer prevents the non-specific adsorption of proteins (Figure 3c). Remarkably, no aggregation of an equimolar suspension of p53- and p14-PEG-calix-AgNPs was observed one hour after the addition of 50% of human serum (Figure 3c). This result highlights the strong robustness of the PEGylated calixarene-coated AgNPs in a complex medium as well as the high selectivity of the sensing system, as only Mdm2 seems capable of triggering the aggregation of the nanoparticles. UV-Vis spectra of all these control experiments can be found in the Supporting Information (Figures S4 to S9). The limit of detection of the sensing system was then determined by using different concentrations of Mdm2 (from 5 to 50 nM). The difference in the ratios of the absorbance at 560 nm and 490 nm before and 30 minutes after the addition of Mdm2 were measured for all the concentrations and a linear relationship was obtained between 5 and 30 nM ($R^2 = 0.9602$) (Figure 4). This result shows the potential of this system as a quantitative colorimetric sensor for Mdm2 at a nanomolar concentration. For concentrations above 30 nM, the sensing system starts to saturate, and a plateau is reached. However, naked eye detection is still possible. It is worth mentioning that with this improved AgNPs-based system, the limit of detection was decreased from 30 nM to 5 nM compared to the previous AuNPs-based sensing system using similar detection conditions (OD of the suspension).

Mdm2 detection in human serum

Finally, the detection of 30 nM Mdm2 was investigated in 50% human serum instead of Tris.HCl buffer. Modifications of the LSPR band of the particles were clearly observed upon addition of Mdm2 (Figure 5). The ratio of absorbances was slightly lower (~0.4 vs ~0.5) than what was obtained in buffer, indicating that the double recognition of Mdm2 by the particles is only weakly hindered when performed in a complex media such as human serum. Again, this highlights the high specificity and robustness of our sensing system. To our knowledge, it represents the first example of a biosensor combining silver nanoparticles and peptides aptamers that can detect a human cancer biomarker in conditions mimicking a real biological sample.

Conclusion

In this work, we used peptide aptamer coated silver nanoparticles as a colorimetric sensor for the oncoprotein Mdm2.[41] This development was possible thanks to the remarkable stability provided by the newly developed calixarene-based coating that allows to covalently conjugate biomolecules on AgNPs and to work in human serum without loss of colloidal stability. Furthermore, the thinness of the coating combined with the small size of the detection ligands (peptide aptamers) makes these particles suitable for the elaboration of colorimetric sensors. Our experiments show that calixarene-coated AgNPs functionalized with peptide aptamers are capable of selectively recognizing the Mdm2 protein. The dual trapping strategy is highly selective, as only the presence of Mdm2 can trigger the aggregation of the two sets of AgNPs. Even when dispersed in human serum, the AgNPs do not aggregate, indicating that the

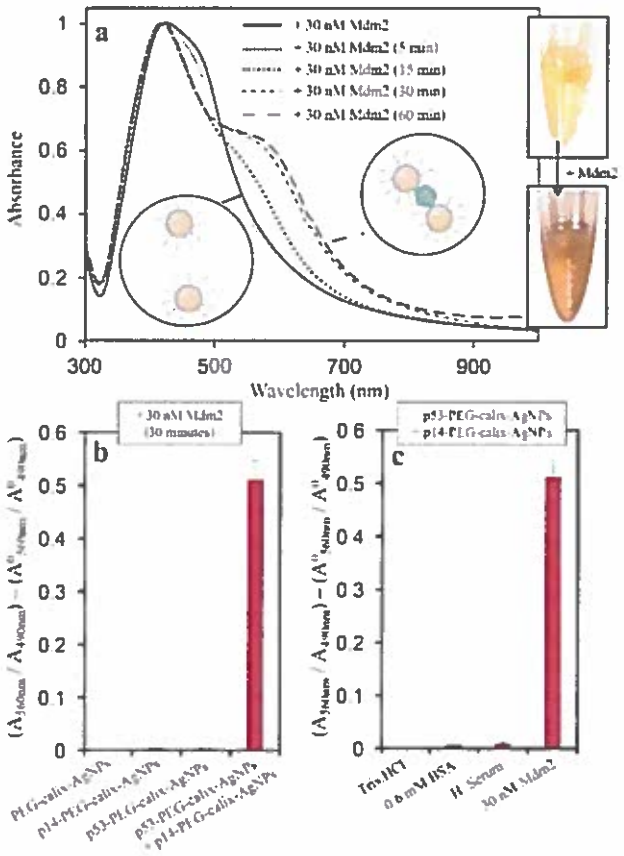

Figure 3. (a) UV-Vis spectra of equimolar suspension of p53-AgNPs and p14-AgNPs in Tris.HCl buffer before and 5, 15, 30 and 60 minutes after the addition of 30 nM Mdm2. Inset: pictures of an equimolar suspension of p53-AgNPs and p14-AgNPs before (top) or after (bottom) the addition of 30 nM of Mdm2. (b) $\Delta A_{560nm}/A_{490nm}$ of a suspension of PEG-calix-AgNPs; p14-PEG-calix-AgNPs; p53-PEG-AgNPs or an equimolar mixture of p14-PEG-calix-AgNPs and p53-PEG-AgNPs before and 30 minutes after the addition of 30 nM of Mdm2. (c) $\Delta A_{560nm}/A_{490nm}$ of a suspension of an equimolar suspension of p14-PEG-calix-AgNPs and p53-PEG-AgNPs before and after the addition of Tris.HCl buffer; 600 μM BSA in Tris.HCl buffer; 50% (vol.) of human serum or 30 nM Mdm2 in 50% of human serum.

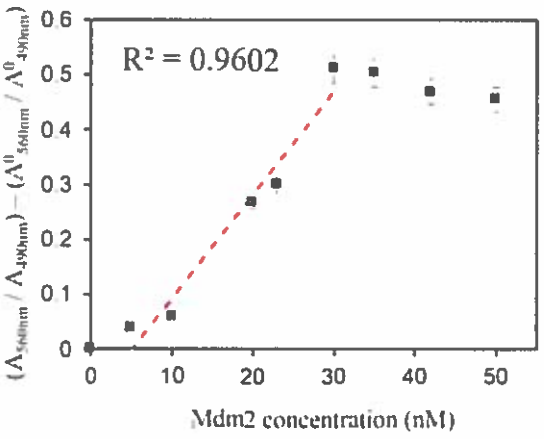

Figure 4. $\Delta A_{560nm}/A_{490nm}$ of an equimolar suspension of p53-PEG-calix-AgNPs and p14-PEG-calix-AgNPs as a function of the concentration of Mdm2.

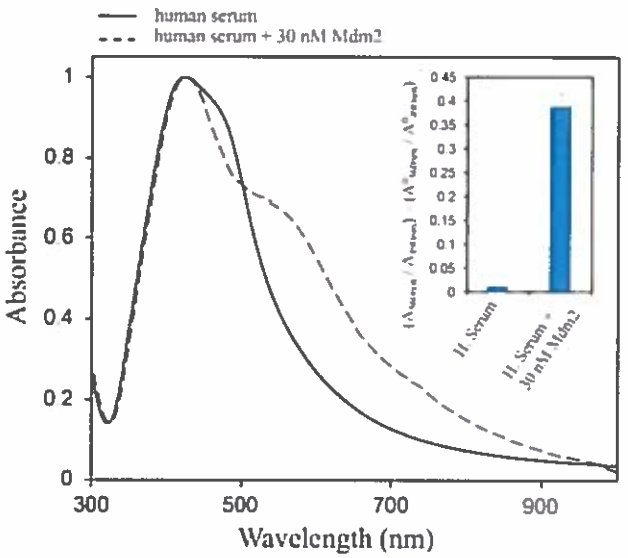

Figure 5. UV-Vis spectra of an equimolar suspension of p53-PEG-calix-AgNPs and p14-PEG-calix-AgNPs after the addition of either 50% human serum (black plain line) or 50% human serum containing 30 nM of Mdm2 (black dashed line). Inset shows the corresponding $\Delta A_{560nm}/A_{490nm}$.

PEGyalted-calixarene layer maintains the particle colloidal stability in a complex biological medium. We have demonstrated that using AgNPs instead of AuNPs improves the limit of detection of the system by almost one order of magnitude. To our knowledge, this is the first time that AgNPs are functionalized with peptide aptamers and used for the colorimetric detection of a cancer biomarker in conditions that mimic real testing conditions. We do believe that this work could pave the way to the development of many other biosensing systems based on AgNPs and a dual-trapping strategy.

Experimental Section

General materials: $AgNO_3$ were purchased from VWR Chemical (Radnor, Pennsylvania). P53 and p14 peptides were ordered from Eurogentec. Human serum (088HSER) was ordered from Zenbio (New-York, NY). Sodium ascorbate, 1-ethyl-3-(3-(dimethylamino)propyl) carbodiimide hydrochloride (EDC) and N-hydroxysulfosuccinimide (Sulfo-NHS) were ordered from Sigma-Aldrich (Saint-Louis, Missouri). Sodium n-dodecyl sulfate were purchased from Alfa Aesar (Kandel, Germany). The PEGylated calixarene-tetradiazonium salt was synthesized according to procedures reported in the literature.[57] Before use, all glassware and Teflon-coated stir bars were washed with aqua regia (3:1 volume ratio of concentrated HCl and HNO_3) and rinsed thoroughly with water.

Caution! Although we have not encountered any problem, it is noted that diazonium salt derivatives are potentially explosive and should be handled with appropriate precautions. Aqua regia is highly toxic and corrosive and requires proper personal protective equipment. Aqua regia should only be handled in a fume hood.

Measurements: UV-Vis absorption spectra were recorded from 1000 to 300 nm at a 120 nm/min scan speed with a UV-Vis-NIR spectrophotometer in disposable (PMMA) cuvettes with a 1 cm optical path length at room temperature. Samples were charac-

terized by dynamic light scattering (DLS) with backscattering (NIBS 173°). Measurements were performed at 25 °C using a refractive index of 1.54 for the gold nanoparticles. AgNPs (20 μL, A ~ 5) were dispersed in lichrosolv water to obtain 1 mL of AgNPs (A ~ 0.1 nM) in disposable semi-micro cuvettes (PMMA) and multiple (>5) DLS measurements were performed. The reported values are the average hydrodynamic diameters obtained from three independent measurements using the Z average as calculated by the Zetasizer software. Attenuated Total Reflection Fourier-transform Infrared (ATR-FTIR) spectra were recorded at 22 °C on a FTIR spectrophotometer equipped with a liquid-nitrogen-cooled mercury-cadmium-telluride detector. The spectrophotometer was continuously purged with dried air. The AgNPs were deposited in solution on a germanium single-crystal internal reflection element (triangular prism of 6.8×45 mm, with an internal incidence angle of 45°), and the solvent was removed with a flow of nitrogen gas. Bare germanium was used for the background spectrum. Opus software (4.2.37) was used to record 128 scans with a nominal resolution of 2 cm^{-1}. Data were processed and analyzed using the home written Kinetics package in Matlab R2013a by subtraction of water vapor, baseline correction, and apodization at 10 cm^{-1}. Images of the AgNPs were obtained with a Philips CM20-UltraTWIN Transmission Electron Microscope (TEM) equipped with a lanthanum hexaboride (LaB6) crystal at a 200 kV accelerating voltage. The average size and 95% confidence interval were determined by measuring the size of more than 100 AgNPs.

Synthesis of PEG-calix-AgNPs: 150 μL of an aqueous solution of $AgNO_3$ (10 mM) were mixed with 575 μL of lichrosolv water and 360 μL of an aqueous solution of PEGylated calixarene-tetradiazonium salt (5 mM). The pH was increased to 7 through the addition of an appropriate volume of NaOH 1 M. Quickly after this, 410 μL of an aqueous solution of sodium ascorbate (15 mM) were added and the resulting solution was stirred for 16 hours at 60 °C. After ca. 10 minutes, a change of color of the solution can be clearly observed, becoming yellow. The nanoparticles were then washed through centrifugation. Briefly, the NPs were centrifuged at 20,000 g for 20 minutes, the supernatant was removed and replaced by SDS 1% (mass.). This process was repeated two times then two other cycles were performed with replacement of the supernatant by pure water. Four cycles were then performed in order to completely discard all the unreacted reagents as well as small and non-coated particles. It is worth mentioning that the first supernatant was yellow due to the presence of small particles that do not precipitate in these centrifugation conditions.

Conjugation of p53- and p14-peptide to PEGylated calixarene-coated AgNPs: In a 1.5 mL Protein LoBind Eppendorf, PEG-calix-AgNPs were diluted in MES buffer for the p53-peptide (10 mM, pH 5.8) or in Borate buffer (20 mM, pH 9) for the p14-peptide in order to reach a concentration of 1 nM in nanoparticles (Abs. = 5) in a volume of 500 μL. A lysine residue was added to the C-terminal extremity of the p14 peptide to allow bioconjugation, while the lysine residue of the p53 peptide was also protected leaving its N-terminal extremity as single anchoring point. To this, 10 μL of an aqueous solution of EDC (6 mM) and 10 μL of an aqueous solution of Sulfo-NHS (10 mM) were added. The resulting suspensions were stirred at room temperature for one hour to activate the carboxyl groups carried by the particles. After one hour, 1 mL of pure water was added, and the particles were centrifuged at 20.000 g for 20 minutes, the supernatant was discarded and replaced by 450 μL of pure water. Ultrasonication could be necessary to resuspend the particles but was not systematically performed. Finally, an appropriate volume of the peptide aptamer (either p14 or p53) was added in order to reach 5000 equivalents per particle and the final solution was stirred for 4 hours at room temperature. The particles were then cleaned from excess of reagents and adsorbed peptides via centrifugation cycles. One cycle involving replacement of the supernatant with SDS 1% in mass to ensure the removal of adsorbed peptides was performed, followed by 2 cycles with pure water to discard any residual reactant.

Mdm2 detection in buffer. In a Protein LoBind Eppendorf, 6 μL of a suspension of p53-PEG-calix-AgNPs (Abs. = 5) were mixed with 6 μL of a suspension of p14-PEG-calix-AgNPs (Abs. = 5) and 108 μL of Tris.HCl. A UV-Vis spectrum of the resulting suspension was recorded. To this, an appropriate volume of Mdm2 (250 nM, Tris.HCl) was added in order to obtain the final desired Mdm2 concentration and a UV-Vis spectrum was recorded after 30 minutes.

Mdm2 detection in human serum. In a Protein LoBind Eppendorf, 6 μL of a suspension of p53-PEG-calix-AgNPs (A = 5) were mixed with 6 μL of a suspension of p14-PEG-calix-AgNPs (A = 5) and 108 μL of Human serum. To this, an appropriate volume of Mdm2 (250 nM, Tris.HCl) was added in order to obtain the final desired Mdm2 concentration and 30 minutes later, the resulting suspension was centrifuged in order to remove the human serum and a UV-Vis spectrum was recorded and compared to the initial one of the particles.

Acknowledgements

The "Actions de Recherches Concertées" of the Fédération Wallonie-Bruxelles and the ULB (Ph.D. grant to M. R.) are acknowledged for financial support.

Conflict of Interest

M. R. was a postdoctoral researcher for X4C from August 2020 to January 2021. I. J. is a shareholder of X4C. I. J. and G.B. are consultants for X4C.

Keywords: calixarenes · colorimetric detection · oncoproteins · peptide aptamers · silver nanoparticles

[1] A. B. Chinen, C. M. Guan, J. R. Ferrer, S. N. Barnaby, T. J. Merkel, C. A. Mirkin, *Chem. Rev.* **2015**, *115*, 10530–10574.
[2] X. C. Magdalena Swierczewska, Gang Liu, Seulki Lee, *Chem. Soc. Rev.* **2011**, *23*, 1–7.
[3] T. Reuveni, M. Motiei, Z. Romman, A. Popovtzer, R. Popovtzer, *Int. J. Nanomed.* **2011**, *6*, 2859–2864.
[4] P. Sandbhor Gaikwad, R. Banerjee, *Analyst* **2018**, *143*, 1326–1348.
[5] L. Syedmoradi, M. L. Norton, K. Omidfar, *Talanta* **2021**, *225*, 122002.
[6] M. J. Daniels, Y. Wang, M. Lee, A. R. Venkitaraman, *Science* **2004**, *306*, 876–879.
[7] J. F. Masson, T. M. Battaglia, P. Khairallah, S. Beaudoin, K. S. Booksh, *Anal. Chem.* **2007**, *79*, 612–619.
[8] X. Huang, Y. Liu, B. Yung, Y. Xiong, X. Chen, *ACS Nano* **2017**, *11*, 5238–5292.
[9] R. Wilson, *Chem. Soc. Rev.* **2008**, *37*, 2028–2045.
[10] P. K. Jain, S. Eustis, M. A. El-Sayed, *J. Phys. Chem. B* **2006**, *110*, 18243–18253.
[11] P. K. Jain, X. Huang, I. H. El-Sayed, M. a. El-Sayed, *Plasmonics* **2007**, *2*, 107–118.
[12] K. L. Kelly, E. Coronado, L. L. Zhao, G. C. Schatz, *J. Phys. Chem. B* **2003**, *107*, 668–677.
[13] D. Paramelle, A. Sadovoy, S. Gorelik, P. Free, J. Hobley, D. G. Fernig, *Analyst* **2014**, *139*, 4855–4861.
[14] X. Liu, M. Atwater, J. Wang, Q. Huo, *Colloids Surf. B* **2007**, *58*, 3–7.

[15] M. Cordeiro, F. F. Carlos, P. Pedrosa, A. Lopez, P. V. Baptista, *Diagnostics* **2016**, *6*, 43.
[16] C. Daruich De Souza, B. Ribeiro Nogueira, M. E. C. M. Rostelato, *J. Alloys Compd.* **2019**, *798*, 714–740.
[17] M. H. Jazayeri, H. Amani, A. A. Pourfatollah, H. Pazoki-Toroudi, B. Sedighimoghaddam, *Sensing and Bio-Sensing Research* **2016**, *9*, 17–22.
[18] J. Zhang, L. Mou, X. Jiang, *Chem. Sci.* **2020**, *11*, 923–936.
[19] M. Retout, E. Brunetti, H. Valkenier, G. Bruylants, *J. Colloid Interface Sci.* **2019**, *557*, 807–815.
[20] A. Loiseau, V. Asila, G. Boitel-Aullen, M. Lam, M. Salmain, S. Boujday, *Biosensors* **2019**, *9*, 78.
[21] J. Sun, Y. Lu, L. He, J. Pang, F. Yang, Y. Liu, *TrAC Trends Anal. Chem.* **2020**, *122*, 115754.
[22] J. H. Soh, Y. Lin, S. Rana, J. Y. Ying, M. M. Stevens, *Anal. Chem.* **2015**, *87*, 7644–7652.
[23] F. Xia, X. Zuo, R. Yang, Y. Xiao, D. Kang, A. Vallée-Bélisle, X. Gong, J. D. Yuen, B. B. Y. Hsu, A. J. Heeger, K. W. Plaxco, *Proc. Natl. Acad. Sci. USA* **2010**, *107*, 10837–10841.
[24] A. Chamorro-Garcia, A. de la Escosura-Muñiz, M. Espinoza-Castañeda, C. J. Rodriguez-Hernandez, C. de Torres, A. Merkoçi, *Nanomedicine: Nanotechnology, Biology, and Medicine* **2016**, *12*, 53–61.
[25] C. C. Huang, Y. F. Huang, Z. Cao, W. Tan, H. T. Chang, *Anal. Chem.* **2005**, *77*, 5735–5741.
[26] K. Zhu, Y. Zhang, S. He, W. Chen, J. Shen, Z. Wang, X. Jiang, *Anal. Chem.* **2012**, *84*, 4267–4270.
[27] M. N. Creyer, Z. Jin, C. Moore, W. Yim, J. Zhou, J. v. Jokerst, *ACS Appl. Mater. Interfaces* **2021**, *13*, 45236–45243.
[28] W. Wang, T. Kong, D. Zhang, J. Zhang, G. Cheng, *Anal. Chem.* **2015**, *87*, 10822–10829.
[29] Q. Wang, R. Liu, X. Yang, K. Wang, J. Zhu, L. He, Q. Li, *Sens. Actuators B* **2016**, *223*, 613–620.
[30] S. K. Ghosh, T. Pal, *Chem. Rev.* **2007**, *107*, 4797–862.
[31] L. Guo, Y. Xu, A. R. Ferhan, G. Chen, D. H. Kim, *J. Am. Chem. Soc.* **2013**, *135*, 12338–12345.
[32] A. Lesniewski, M. Los, M. Jonsson-Niedziołåka, A. Krajewska, K. Szot, J. M. Los, J. Niedziolka-Jonsson, *Bioconjugate Chem.* **2014**, *25*, 644–648.
[33] H. Daraee, A. Eatemadi, E. Abbasi, S. F. Aval, M. Kouhi, A. Akbarzadeh, *Artif. Cells, Nanomed., Biotechnol.* **2016**, *44*, 410–422.
[34] B. Kim, S. Choi, S. Han, K.-Y. Choi, Y. Lim, *Chem. Commun.* **2013**, *49*, 7617–9.
[35] C.-C. Chang, C.-Y. C.-P. Chen, C.-H. Lee, C.-Y. C.-P. Chen, C.-W. Lin, *Chem. Commun.* **2014**, *50*, 14443–6.
[36] H.-Z. Lai, S.-G. Wang, C.-Y. Wu, Y.-C. Chen, *Anal. Chem.* **2015**, *87*, 2114–2120.
[37] N. T. Tung, P. T. Tue, T. Thi Ngoc Lien, Y. Ohno, K. Maehashi, K. Matsumoto, K. Nishigaki, M. Biyani, Y. Takamura, *Sci. Rep.* **2017**, *7*, 1–9.
[38] D. T. H. Kim, D. T. Bao, H. Park, N. M. Ngoc, S. J. Yeo, *Theranostics* **2018**, *8*, 3629–3642.
[39] G. Stefan, O. Hosu, K. de Wael, M. J. Lobo-Castañón, C. Cristea, *Electrochim. Acta* **2021**, *376*, 137994.
[40] M. F. Shaikh, W. F. Morano, J. Lee, E. Gleeson, B. D. Babcock, J. Michl, E. Sarafraz-Yazdi, M. R. Pincus, W. B. Bowne, *Ann. Clin. Lab. Sci.* **2016**, *46*, 627–634.
[41] M. Retout, H. Valkenier, E. Triffaux, T. Doneux, K. Bartik, G. Bruylants, *ACS Sens.* **2016**, *1*, 929–933.
[42] J. S. Lee, A. K. R. Lytton-Jean, S. J. Hurst, C. A. Mirkin, *Nano Lett.* **2007**, *7*, 2112–2115.
[43] L. A. Lane, X. Qian, S. Nie, *Chem. Rev.* **2015**, *115*, 10489–10529.
[44] S. Dey, M. Trau, K. M. Koo, *Nanomaterials* **2020**, *10*, 1–15.
[45] J. Neng, Q. Zhang, P. Sun, *Biosens. Bioelectron.* **2020**, *167*, 112480.
[46] T. T. X. Ong, E. W. Blanch, O. A. H. Jones, *Sci. Total Environ.* **2020**, *720*, 137601.
[47] J. Liu, Y. Wen, H. He, H. Y. Chen, Z. Liu, *Chem. Sci.* **2018**, *9*, 7241–7246.
[48] L. Zhou, Y. Wang, R. Xing, J. Chen, J. Liu, W. Li, Z. Liu, *Biosens. Bioelectron.* **2019**, *145*, 111729.
[49] M. Sabela, S. Balme, M. Bechelany, J. M. Janot, K. Bisetty, *Adv. Eng. Mater.* **2017**, *19*, 1–24.
[50] I. Pinzaru, D. Coricovac, C. Dehelean, E. A. Moacă, M. Mioc, F. Baderca, I. Sizemore, S. Brittle, D. Marti, C. D. Calina, A. M. Tsatsakis, C. Şoica, *Food Chem. Toxicol.* **2018**, *111*, 546–556.
[51] Y. Wang, K. Van Asdonk, P. Zijlstra, *Langmuir* **2019**, *35*, 13356–13363.
[52] S. A. Bansal, V. Kumar, J. Karimi, A. P. Singh, S. Kumar, *Nanoscale Adv.* **2020**, *2*, 3764–3787.
[53] N. G. Bastús, F. Merkoçi, J. Piella, V. Puntes, *Chem. Mater.* **2014**, *26*, 2836–2846.
[54] A. Mirzaei, K. Janghorban, B. Hashemi, M. Bonyani, S. G. Leonardi, G. Neri, *J. Nanostruct. Chem.* **2017**, *7*, 37–46.
[55] Y. Gavamukulya, E. N. Maina, A. M. Meroka, E. S. Madivoli, H. A. El-Shemy, F. Wamunyokoli, G. Magoma, *J. Inorg. Organomet. Polym. Mater.* **2020**, *30*, 1231–1242.
[56] G. von White, P. Kerscher, R. M. Brown, J. D. Morella, W. McAllister, D. Dean, C. L. Kitchens, *J. Nanomater.* **2012**, *2012*, 1–12.
[57] Y. Chen, D. Yin, Y. Ma, Z. Bie, Z. Liu, *Anal. Chem.* **2016**, *88*, 8123–8128.
[58] A. Ravindran, M. Elavarasi, T. C. Prathna, A. M. Raichur, N. Chandrasekaran, A. Mukherjee *Sens. Actuators B* **2012**, *166–167*, 365–371.
[59] C. Han, K. Xu, Q. Liu, X. Liu, J. Li, *Sens. Actuators B* **2014**, *202*, 574–582.
[60] D. Xiong, H. Li, *Nanotechnology* **2008**, *19*, 465502.
[61] A. Mattiuzzi, I. Jabin, C. Mangeney, C. Roux, O. Reinaud, L. Santos, J. F. Bergamini, P. Hapiot, C. Lagrost, *Nat. Commun.* **2012**, *3*, 1130.
[62] L. Troian-Gautier, A. Mattiuzzi, O. Reinaud, C. Lagrost, I. Jabin, *Org. Biomol. Chem.* **2020**, *18*, 3624–3637.
[63] M. Retout, I. Jabin, G. Bruylants, *ACS Omega* **2021**, *6*, 19675–19684.
[64] S. Baek, P. S. Kutchukian, G. L. Verdine, R. Huber, T. a. Holak, K. W. Lee, G. M. Popowicz, *J. Am. Chem. Soc.* **2012**, *134*, 103–106.
[65] J. D. Weber, M.-L. Kuo, B. Bothner, E. L. DiGiammarino, R. W. Kriwacki, M. F. Roussel, C. J. Sherr, *Mol. Cell. Biol.* **2000**, *20*, 2517–2528.
[66] P. Blond, R. Bevernaegie, L. Troian-Gautier, C. Lagrost, J. Hubert, F. Reniers, V. Raussens, I. Jabin, *Langmuir* **2020**, *36*, 12068–12076.
[67] M. Retout, P. Blond, I. Jabin, G. Bruylants, *Bioconjugate Chem.* **2021**, *32*, 290–300.
[68] M. Doyen, J. Goole, K. Bartik, G. Bruylants, *J. Colloid Interface Sci.* **2016**, *464*, 60–166.

Manuscript received: October 7, 2021
Revised manuscript received: December 17, 2021
Accepted manuscript online: December 20, 2021